

**THE GAS TEMPERATURE DIAGNOSTICS BY MEANS OF
AIO ($B^2\Sigma^+ - X^2\Sigma^+$) MOLECULAR BAND SYSTEM FROM THE UPGRADED
ATMOSPHERIC PRESSURE PULSED DISCHARGE SOURCE IN ARGON**

JOVICA JOVOVIĆ¹ and GORDANA LJ. MAJSTOROVIĆ²

¹*Faculty of Physics, University of Belgrade – Studentski trg 12-16,
11000 Belgrade, Serbia
E-mail jjovica@ff.bg.ac.rs*

²*University of Defence, Military Academy, Generala Pavla Jurišića Šturma 33,
Belgrade, Serbia
E-mail gordana.majstorovic@va.mod.gov.rs*

Abstract. In this study, the optical emission spectroscopy (OES) is applied to measure gas temperature from the upgraded needle-to-cylinder (UNTC) gas discharge source in argon driven by pulsed voltage power supply. The rotational T_{rot} temperature is obtained after the analysis of well resolved AIO ($B^2\Sigma^+ - X^2\Sigma^+$) molecular bands at 484.2 nm and 486.6 nm ($\Delta v=0$). The T_{rot} is measured for different pulse width and duty cycle values as well. The Fortrat parabolas were constructed for the proper identification of P_2 and R_2 branch lines belonging to AIO ($B^2\Sigma^+ - X^2\Sigma^+$) molecular bands. The results revealed $T_g \sim 1450-1800$ K in the center of plasma column.

1. INTRODUCTION

The formation of metal-oxide layers (AlO, Al₂O₃, TiO etc.) in plasma-assisted processes comprises several steps such as the evaporation of electrode/target material, reaction with oxidizing particles in plasma and in afterglow and surface reactions. The Plasma Electrolytic Oxidation (PEO) and Plasma Enhanced Atomic Layer Deposition (PE-ALD) are the examples of two approaches in deposition of high-performance oxide layers. The experimental study of metal-oxide molecules contributes to plasma computation, plasma chemistry, radiative lifetimes measurements and collision quenching study (Parriger and Kornhol 2011, Johnson et al 1972, Salzberg et al 1991). In the area of astrophysics, the extensive study of molecular bands originating from the solar spectrum such as MgH, MgO, AIO, CN etc. is made (Schadee 1964 and references therein).

An interesting peculiarity of the UNTC source is the formation of di-atomic molecules in plasma such as NH, OH, AIO and CN. Having that in mind, the focus of this study is on T_g measurement by means of T_{rot} diagnostics procedure based on

normalized population distribution technique using the rovibrational distribution of $\text{AlO} (\text{B}^2\Sigma^+ - \text{X}^2\Sigma^+, 0-0)$ and $\text{AlO} (\text{B}^2\Sigma^+ - \text{X}^2\Sigma^+, 1-1)$ molecular bands. In high pressure regime, being one of the limiting cases discussed in Bruggeman et al 2014, the measured rotational temperature equals gas temperature (rotational energy transfer occurs much faster than depopulation rate of excited level).

2. EXPERIMENTAL

The schematic drawing of UNTC source and experimental setup is shown in Figure 1. The source consists of needle-type cathode (diameter 4 mm) and a cylindrical graphite anode (diameter 25 mm). The cathodes are made of aluminum (0.5 % Mg, 0.5 % Si, 0.5 % Fe and Al balance). The working gas (Ar 99.999 %) flow is measured using rib-guided glass tube flowmeter controller (0-2.5 l/min scale). The discharge is driven by pulsed voltage power supply that consist of DC power supply (Kepco, 0-2 kV, 0-100 mA), the bank of capacitors, HV switching unit (MOSFET technology) and rectangular pulses generator (2-999 μs pulse width, 0.1-100 % duty cycle), see Figure 1 in Jovović 2020. The pulsed power voltage signal, is monitored by means of 4-channel digital oscilloscope (Hantek, $f \leq 250$ MHz, 1.4 ns rise time). During the pulse, the voltage jumps in the range 900-1300 V for 16.7 % duty cycle and 500-600 V for 3.8 % duty cycle. The radiation from UNTC source was recorded by means of 2 m Ebert type spectrometer (Carl Zeiss, O.P. $f/28$, an inverse linear dispersion of 0.74 nm/mm) equipped with a thermoelectrically cooled, back-thinned Hamamatsu CCD camera ($T = -10^\circ\text{C}$, 2048×512 pixels, $12 \mu\text{m}$ pixel size).

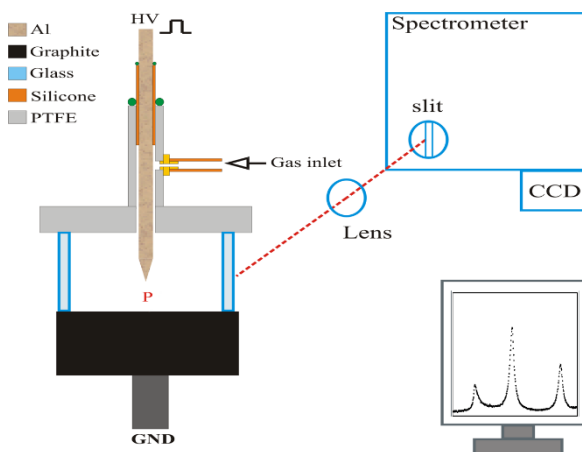


Figure 1: The cross-section of UNTC discharge source and experimental setup.

3. RESULTS AND DISCUSSION

The P_2 branch lines of the $\text{AlO} \text{B}^2\Sigma^+ (v'=0) - \text{X}^2\Sigma^+ (v''=0) (J'=17-35)$ are studied while the R_2 branch lines $\text{AlO} \text{B}^2\Sigma^+ (v'=1) - \text{X}^2\Sigma^+ (v''=1) (J'=33-49)$ transition in the

range 484–488 nm are analyzed as well (Figures 2 and 3) using the procedure and spectroscopic constants listed in Herzberg 1950. Having in mind that rotational transfer coefficients become negligible if ΔE is much higher than average kinetic energy of neutrals $E_{kin} (=kT)$, ΔE has to be the same order of magnitude as E_{kin} (Barbeau et al 1991). In our case, for AIO $B^2\Sigma^+$ ($\nu' = 1$), the energy gap between $J' = 33$ and $J' = 49$ rotational levels is $\Delta E = 914 \text{ cm}^{-1}$ and AIO $B^2\Sigma^+$ ($\nu' = 0$) the energy gap between $J' = 17$ and $J' = 35$ rotational levels is $\Delta E = 574 \text{ cm}^{-1}$. For T_{rot} values of e.g. 1520 K and 1780 K, kT_{rot} equals 1057 cm^{-1} , or 1238 cm^{-1} , respectively. Hence, one may consider the upper levels within abovementioned J' range, to be in equilibrium with molecular ground state (Launila and Berg 2011).

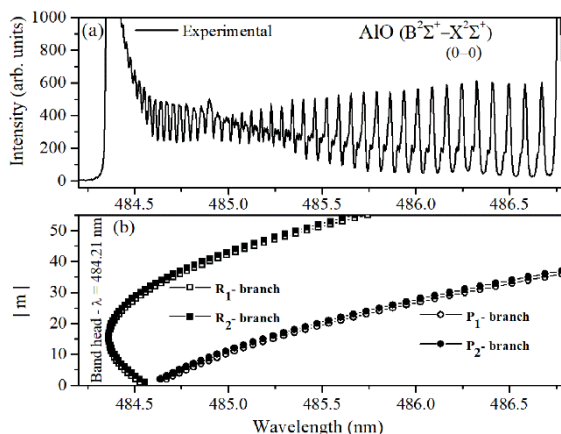


Figure 2: (a) The AIO (0–0) band at 484.2 nm recorded in the second order of diffraction grating. (b) Fortrat parabolas of the main branches of the AIO (0–0) spectrum (m designates the number of successive lines in each branch).

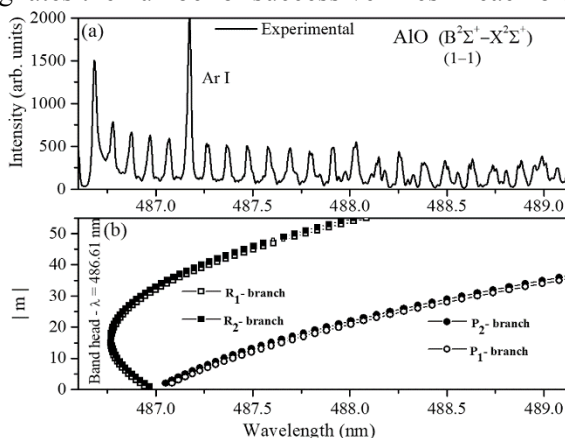


Figure 3: (a) The AIO (1–1) band at 486.6 nm recorded in the second order of diffraction grating. (b) Fortrat parabolas of the main branches of the AIO (1–1) spectrum (m designates the number of successive lines in each branch).

Let us mention that, for different values of pulse width (50 μs , 100 μs and 300 μs) and duty cycle (25 %, 16.7 %, 9.1 % and 4.75 %), the T_{rot} was measured using AIO ($\text{B}^2\Sigma^+ - \text{X}^2\Sigma^+$, 0–0) and AIO ($\text{B}^2\Sigma^+ - \text{X}^2\Sigma^+$, 1–1) bands as well, see Table 1. It was observed that lowering of the duty cycle induces the lowering of T_{rot} which reflects the change of T_{g} in plasma. It is reasonable to claim that power supply with shorter pulse width and lower pause/pulse ratio delivers the higher power into the plasma volume and consequently increases the efficiency of neutral particles heating.

AIO (0–0)	50 μs	100 μs	300 μs
25 %	1640 \pm 165	1640 \pm 165	1780 \pm 180
16.7 %	1590 \pm 160	1590 \pm 160	1700 \pm 170
9.1 %	1440 \pm 145	1400 \pm 140	1710 \pm 175
4.75 %	1300 \pm 130	1300 \pm 130	1620 \pm 165
AIO (1–1)	50 μs	100 μs	300 μs
25 %	1480 \pm 150	1540 \pm 155	1520 \pm 155
16.7 %	1460 \pm 150	1530 \pm 155	1420 \pm 145
9.1 %	1440 \pm 145	1510 \pm 155	1550 \pm 155
4.75 %	1600 \pm 160	1920 \pm 195	1610 \pm 165

Table 1: The change of T_{rot} (K) with pulse width and duty cycle.

Acknowledgement

This work is supported by the Ministry of Education, Science and Technological Development of the Republic of Serbia.

References

- Parigger, C. G., Kornhol, J. O. M. : 2011, *Spectrochim. Acta A*, **81**, 404.
 Johnson, S. E., Capelle G. and Broida H. P. : 1972, *J. Chem. Phys.*, **56**, 663.
 Salzberg, A. P., Santiago, D. I., Asmar, F., Sandoval, D. N. and Weiner, B. R. : 1991, *Chem. Phys. Lett.*, **180**, 161.
 Schadee, A. : 1964, *Bulletin of the Astronomical Institutes of the Netherlands*, **17**, 311.
 Bruggeman, P. J., Sadeghi, N., Schram, D. C. and Linss, V. : 2014, *Plasma Sources Sci. Technol.*, **23**, 023001.
 Jovović, J. : 2020, *Phys. Plasmas*, **27**, 053505.
 Herzberg, G. : 1950, *Molecular spectra and molecular structure, vol I*, Van Nostrand-Reinhold, New York.
 Barbeau, C., Baravian, G., and Jolly, J. : 1991, *Proceedings of X International Symposium on Plasma Chemistry*, Bochum.
 Launila, O., Berg, J.-E. : 2011, *J. Mol. Spectroscopy*, **265**, 10.